DOI: 10.1784/insi.2018.60.8.XXX

NDE sensor delivery using unmanned aerial vehicles

R Jarvis, A Farinha, M Kovac and F Cegla

The robotic deployment of NDE sensors has great cost-saving potential in cases where the measurement cost is high due to access restrictions or the need to temporarily decommission the test structure. Unmanned aerial vehicles (UAVs) are able to quickly reach inaccessible components to perform visual inspection and deploy NDE sensors. In this work, a mechanical sensor release mechanism is presented that has enabled electromagnetic acoustic transducers (EMATs) to be deployed onto a ferromagnetic pipe and a plate, after which the component wall thickness measurements can be transmitted wirelessly to a remote location. The reliability of the method and the most promising areas for future development are discussed.

Keywords: automated and robotic NDT, research, petroleum industry, EMAT, condition monitoring, accuracy and reliability.

Introduction

Non-destructive evaluation (NDE) sensors provide information about the structural integrity of a component, which can ensure its continued safe operation, avoid the cost of its premature replacement or enable efficient planning for component replacement to minimise lost production. Ultrasonic thickness measurements are commonly carried out to identify time-dependent degradation such as internal corrosion or erosion, which may not be identified by visual inspection alone. In the oil & gas sector, electromagnetic acoustic transducers (EMATs) are ideally suited to carry out these measurements as, unlike piezoelectric transducers, they do not require couplant. EMATs function with little to no surface preparation and the magnetic forces result in a form of self-adhesion on ferromagnetic components.

Conventional EMATs require high-power excitation; however, the NDE Group at Imperial College London has been involved in the optimisation of EMATs[1] and acquisition methodologies[2], which has made it possible to produce intrinsically safe EMATs. Commercial systems exist for the permanent installation of a network of EMAT sensors on components such as facility pipework, which provide frequent wall thickness readings and wireless acquisition of the data for structural health monitoring (SHM)[3]. The amount of data provided using SHM increases the accuracy and reliability of wall thickness readings in comparison to periodic one-off inspections and enables accurate predictions of the remnant life of the component.

The cost of installing NDE sensors such as EMATs in petrochemical facilities frequently exceeds the measurement cost. Pressure components within an oil & gas facility can have access issues, necessitating scaffolding construction before operators can perform a visual inspection of the component and deploy the NDE sensors. In many cases, the component must be temporarily decommissioned to ensure the safety of service personnel at the expense of lost production[4,5]. In these scenarios, there is a clear cost-saving potential associated with using unmanned aerial vehicles (UAVs) to perform the visual inspection as well as deploy NDE sensors.

Within the engineering sector, the unique viewpoint offered by UAVs has been the motivation for their use in infrastructure monitoring via on-board cameras that can be visual, infrared or multi-spectral[6]. Within the field of NDE, the ability of UAVs to reach difficult-to-access locations has been particularly advantageous in cases where access or temporary decommissioning costs exceed the measurement cost. Example applications of visual and thermographic imaging include: concrete bridge decks without suspending traffic[7,8]; storage tanks; power lines; cooling towers; elevated pipes[9]; concrete chimneys[10]; wind turbine rotor blades[11]; and photovoltaic plants[12]. In many cases, UAV inspection is much quicker than the equivalent inspection involving human operators. Air-coupled ultrasonic sensors have been employed on UAVs for collision detection purposes[13,14]; however, the use of ultrasonic sensors for NDE purposes is less common. At the time of writing, there exists only a single company claiming the capability to perform UAV-deployed ultrasonic thickness measurements[15]. It is claimed that the piezoelectric sensor can be deployed with a positional accuracy of 10 mm and requires a couplant stored within a tank on the UAV.

To the best of the authors' knowledge, there have not been any documented attempts to deploy sensors for SHM using UAVs; however, the use of robotic manipulators for aerial interaction or the pick-and-place of objects continues to be a popular research topic[16-22]. It remains a challenge to stabilise and optimise the aerial dynamics of the system in response to a payload, especially if it can swing on a tether below the UAV[17,23-28].

In this paper, the remote deployment of NDE sensors is explored. Although applications exist across the NDE industry, the focus is placed on the oil & gas industry as the potential cost savings are large. This paper first outlines the experimental methods, followed by the presentation and discussion of the results that were obtained. The paper ends with a short conclusion.

● ***Submitted 23.01.18 / Accepted 22.05.18***

Rollo Jarvis and Frederic Cegla are with the Department of Mechanical Engineering, Imperial College London, Exhibition Road, South Kensington, London SW7 2AZ, UK.*

Mirko Kovac and Andre Farinha are with the Department of Aeronautics, Imperial College London, Exhibition Road, South Kensington, London SW7 2AZ, UK.*

**Corresponding authors. Email: f.cegla@imperial.ac.uk (mechanical) / m.kovac@imperial.ac.uk (UAV)*

Methodology

In this preliminary work, a fully mechanical sensor holder was designed due to its relative simplicity and short development time in comparison to an electronically actuated gripper. After the magnetic adhesion of the sensor to the ferromagnetic structure, minimal force is required to overcome the friction between the arms and open the holder. Low-impact deployment is important to make the design compatible with the requirements of the safety-critical oil & gas sector. The authors estimate that the force exerted by the UAV onto the pipe structure in order to release the sensor is much less than the force that the structure experiences during the magnetic attachment of the sensor; however, flying a UAV close to the structure will require favourable piloting skills and environmental conditions as well as protection mechanisms around the UAVs moving parts, which have previously been developed for visual inspection tasks. In the prototype design shown in Figure 1, two 'C' shaped arms are connected to short struts and joined with a pin in two places along the vertical axis. This mechanism causes the arms to be held in a closed state due to the weight of the sensor. An upward force on the top of the arms results in them opening, allowing the sensor to be released. This behaviour ensures that the sensor is always secured during flight, as even severe tilting of the UAV does not exert an upwards force that exceeds the weight of the sensor. An aluminium guide was used to prevent the sensor from swinging and negatively affecting the flight stability. The design was prototyped in LEGO® Technic and later 3D printed, as rendered in Figure 2. The sensor deployment methodology is inspired by the way that flies land on vertical surfaces[29]. Instead of using complex sensing and navigation to coordinate the landing motion, the fly extends its legs to dampen the impact, allowing for a robust landing. Similar in concept, compliant mechanical structures are used here that cushion the impact and release the sensor on contact, using solely mechanical means.

The sensor-carrying mechanism was attached to a Tarot TL65B01 frame with a DJI propulsion system (four 310 kV DJI 4216 motors with a recommended maximum payload of 2.25 kg), but similar systems would also be suitable. The UAV was designed for use with two batteries, although only one was used to reduce the overall weight. This provided a total potential flight time of approximately 7-11 min when carrying the sensor. The UAV was piloted manually, beginning on a stand with the sensor attached before flying 3 m to deploy the sensor onto the target. Two targets were selected. Firstly, the centre of a 1.3 m^2, 1.5 mm-thick steel plate and, secondly, the halfway point on a 275 mm length of 6" schedule-40 pipe. For a length of 75 mm about the pipe centre, the 7.1 mm wall thickness was reduced from the inner wall by 2 mm to simulate an inner-wall thinning defect (for example erosion or non-pitting corrosion). A line scan of the pipe wall was completed using an EMAT (Innerspec PE-L-B-0.726-0.492 butterfly coil with a 274A0244 magnet[30]) at 4 MHz, to allow for comparison with the UAV-deployed EMAT measurements.

An ET210 EMAT sensor for aerial deployment was provided by Permasense Ltd[3]. The ET210 contains a coil and magnet, a battery and a wireless transmission module. Its relatively high mass of 667 g is due to the casing infill required to meet intrinsic safety standards for operation in a petrochemical environment. Once installed, the sensor can operate for multiple years. Figure 3 shows the sensor, placed on the top of the pipe target, transmitting temperature-compensated wall thickness readings to a laptop via a wireless gateway. Ten attempted landings were performed on the plate target, which was primarily used to practice the control of the UAV, as deployment of the sensor on a flat horizontal surface was simpler than on a curved structure. Immediately afterwards, the target was replaced with the pipe and the experiment was repeated until ten successful attempts were recorded. A video recording was made of each attempt and the final sensor position and flight time were recorded.

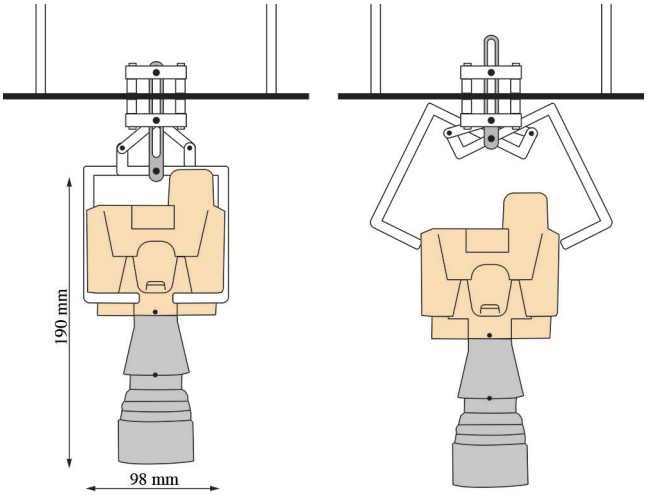


Figure 1. Schematic of the mechanical sensor holder in closed (left) and open (right) positions. Dimensions of the 667 g Permasense ET210 EMAT sensor are shown

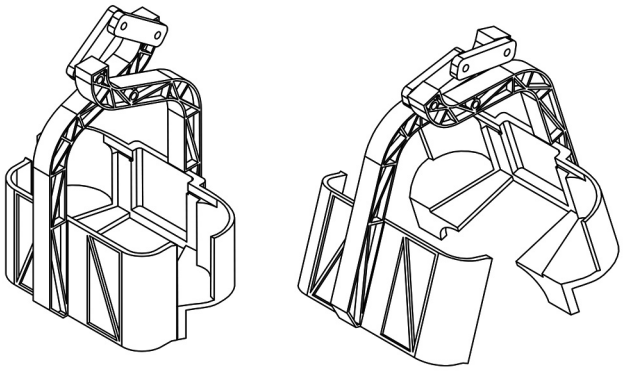


Figure 2. A rendering of the 3D printed prototype sensor holder

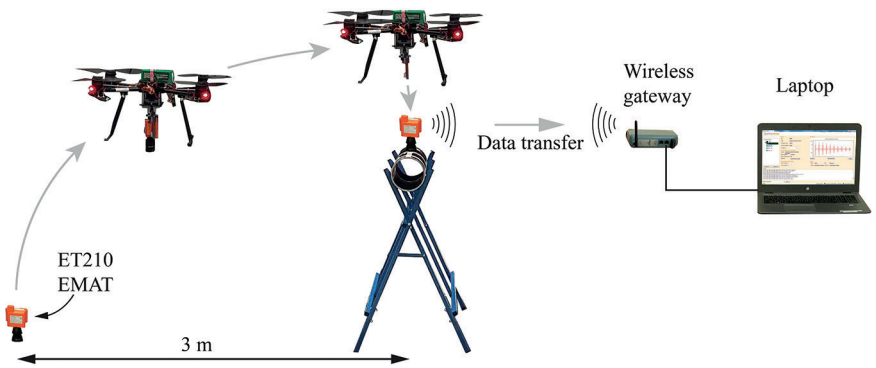


Figure 3. The Permasense ET210 EMAT sensor, which is transported by the UAV to the pipe sample, transmits data to a PC via a wireless gateway

For the pipe target, the wall thickness of the pipe sample was recorded wirelessly after the sensor was deployed. The thickness of the plate was not recorded as it was thinner (<3 mm) than the minimum thickness that can be measured using the ET210 wireless thickness sensor.

Results and discussion

Figure 4 shows the stages of deployment onto the plate. A successful deployment rate of 65% was recorded. Each unsuccessful landing was due to the landing trajectory not being perpendicular to the target, resulting in the magnetic part of the sensor not making contact with the plate and preventing magnetic adhesion of the sensor. The magnetic force was limited due to a steel thickness of just 1.5 mm, suggesting that more tilt could be tolerated when deploying the sensor to thicker-walled components. Examples of unsuccessful landings due to tilt are shown in Figure 5. The sensor was not prematurely released during flight in any of the landing attempts. For the pipe target, a similar success ratio of 60% was recorded despite the potential target being much smaller due to the pipe curvature. Figure 6 shows the stages of successful deployment onto the pipe. The unsuccessful cases were once again due to the sensor landing off-target. As the UAV was manually controlled, it was challenging to approach the target in a slow and controlled manner. Valuable future work should optimise the control method within an industrial setting. For example, a visual navigation system will enable a much more accurate and controlled flight trajectory; however, it may be challenging to implement in a practical environment outdoors due to complex and changing environmental conditions.

Figure 7 shows the landing locations of the sensor relative to the target location on both the pipe and the plate. The mean and standard deviation of the distance to the target centre were 0.21 m and 0.23 m for the plate and 0.13 m and 0.04 m for the pipe, respectively. The apparent accuracy increase on the pipe is likely to be due to the decreased area available for landing; however, it is important to stress that these metrics are influenced strongly by the ability of the pilot (it should be noted that the pilot did not practice for longer than a few minutes before the experiment). Therefore, they do not give a strong indication of how accurately a sensor could be deployed using manual flight under realistic conditions, nor the robustness and reliability of the mechanical release. These metrics indicate the performance one might expect to achieve in a similar scenario; however, the small sample size and the influence of pilot ability mean that care should be taken when interpreting or comparing these results. The flight times varied between 15-60 s from the moment of take-off until landing after deployment of the sensor. The wall thickness readings shown in Figure 7(b) were recorded wirelessly from the ET210 sensors after deployment and are consistent with the pipe thickness stated by the manufacturer of 7.1 mm within the tolerances of ±12.5%[31]. The transducer response (A-scan) could be downloaded wirelessly from the sensor following deployment. When the back-wall reflections were clearly visible, it was possible to ascertain that the sensors had been installed onto the component (even without a line of sight to the test component).

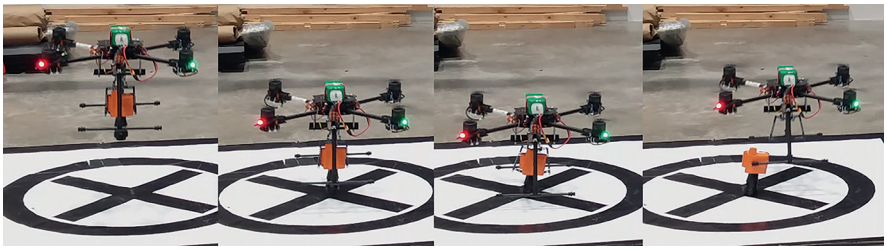


Figure 4. The sensor landing on the plate. A photo sequence showing the approach, landing, release and take-off. 2.5 s elapse between the first and last frames

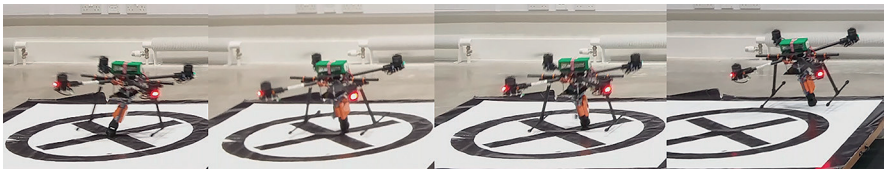
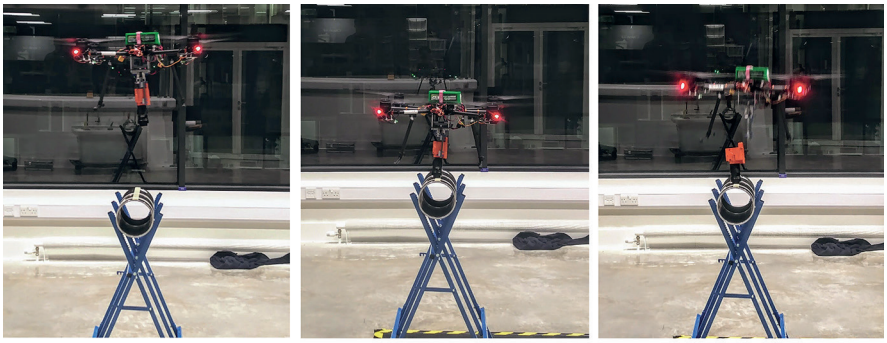


Figure 5. Landing at an angle was the most common reason for a failed deployment, as shown in these examples



(a) **(b)** **(c)**

Figure 6. A photo sequence showing the UAV placing the ET210 EMAT sensor onto the pipe: (a) approach; (b) deployment; and (c) take-off

Figure 8 shows a line scan over the length of the pipe at the 12 o'clock position (marked in Figure 7(b)), completed using a 4 MHz EMAT. The reduced wall thickness region can clearly be seen between 200 mm and 275 mm. The spatial sampling of the line scan was 1 mm and the apparent error at the location of the thickness change is due to small positional misalignments between the repeated scans before averaging. The periodic wall thickness variations seen outside of these regions are due to the seamless pipe manufacturing process[32]. In certain cases, it is important to obtain the spatial distribution of the wall thickness to analyse structural integrity (for example by determining the extent of a damaged area); however, it cannot be measured by immobile sensors that are permanently installed.

In addition to improving the delivery success rate to 100%, a number of challenges must be addressed to further develop the NDE sensor delivery system. This preliminary work only considered the deployment of sensors to the top of a pipe. A future solution should consider how sensors could be placed anywhere around the circumference of the pipe. It would also be advantageous to develop the system for pick-and-place, so that manual

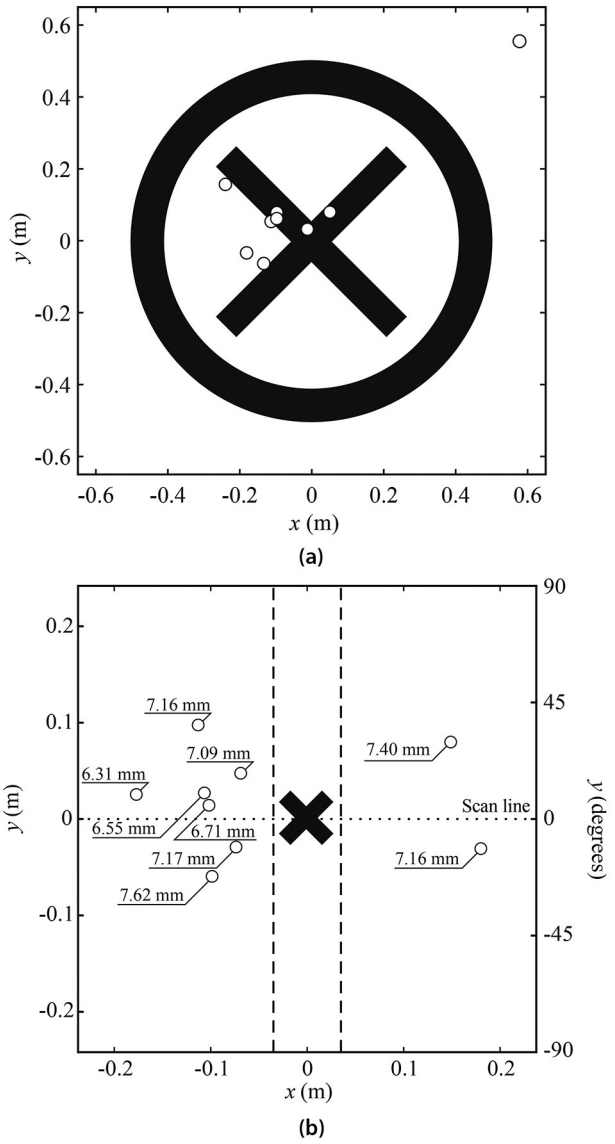


Figure 7. Landing locations of the sensor using manual flight relative to targets marked with an 'X' on: (a) the plate; and (b) the pipe. The area between the dashed lines indicates the region of reduced inner wall thickness and the thicknesses recorded with the ET210 sensor are marked. The dotted line shows the position of the wall thickness line scan

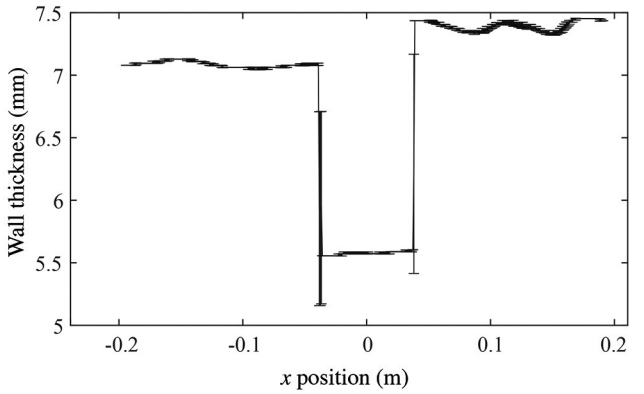


Figure 8. Mean of the wall thickness line-scans completed on the pipe sample with a 4 MHz EMAT. Error bars are the standard deviation on the mean

loading of the sensor would not be required. To achieve these goals, it is likely that an actuated robotic arm would be required in place of a simple mechanism. Additional considerations should be made when developing a system for practical implementation, such as the effect of adverse weather conditions, additional ways to secure the sensor and procedures for aborted landings.

Conclusions

This study has demonstrated that UAVs can be used to deploy NDE sensors, which has great cost-saving potential by replacing human operators in cases where the installation costs are high. A simple mechanical sensor holder attached to a UAV allowed deployment of an EMAT sensor to a ferromagnetic steel plate and pipe located 3 m away in under 30 s when manually controlled by a pilot with no prior experience of the system. A 65% successful deployment rate was recorded for the plate and 60% for the pipe. In the unsuccessful attempts, the sensor could not magnetically adhere to the steel surface due to an angled landing trajectory. The sensor was never prematurely released from the mechanism during flight. This control scheme allowed a deployment accuracy (mean and standard deviation from the target centre) of 0.21 ± 0.23 m for the plate and 0.13 ± 0.04 m for the pipe. The landing trajectory and impact location should be better controlled in order to improve the future performance of the system; this could be achieved using an autopilot control scheme. The mechanism is currently restrained to vertical approach and if sensor placement at 90° or larger is required then different mechanisms should be investigated.

Acknowledgements

This research was funded by grant number EPSRC EP/R026173/1. The authors would like to thank Permasense Ltd for kindly providing the ET210 sensors.

References

1. J Isla and F Cegla, 'Optimisation of the bias magnetic field of shear wave EMATs', IEEE Transactions on Ultrasonics, Ferroelectrics and Frequency Control, Vol 63, No 8, pp 1148-1160, 2016. DOI: 10.1109/TUFFC.2016.2558467. Available at: https://ieeexplore.ieee.org/document/7460084/?arnumber=7460084
2. J Isla and F Cegla, 'Coded excitation for pulse-echo systems', IEEE Transactions on Ultrasonics, Ferroelectrics and Frequency Control, Vol 64, No 4, pp 736-748, 2017. DOI: 10.1109/TUFFC.2017.2661383. Available at: http://ieeexplore.ieee.org/document/7836318/
3. Permasense Inc, www.permasense.com
4. L Marconi, F Basile, G Caprari *et al*, 'Aerial service robotics: the AIRobots perspective', Proceedings of the 2nd International Conference on Applied Robotics for the Power Industry (CARPI 2012), Zurich, Switzerland, pp 64-69, 11-13 September 2012. DOI: 10.1109/CARPI.2012.6473361. Available at: https://ieeexplore.ieee.org/document/6473361/
5. R C Ratnayake, 'Challenges in inspection planning for maintenance of static mechanical equipment on ageing oil and gas production plants: the state-of-the-art', Proceedings of the ASME 31st International Conference on Ocean, Offshore and Arctic Engineering, Rio de Janeiro, Brazil, pp 91-103, 1-6 July 2012. DOI: 10.1115/OMAE2012-83248
6. I Colomina and P Molina, 'Unmanned aerial systems for photogrammetry and remote sensing: a review', ISPRS Journal

of Photogrammetry and Remote Sensing, Vol 92, pp 79-97, 2014. DOI: 10.1016/J.ISPRSJPRS.2014.02.013. Available at: www.sciencedirect.com/science/article/pii/S0924271614000501
7. T Omar and M L Nehdi, 'Remote sensing of concrete bridge decks using unmanned aerial vehicle infrared thermography', Automation in Construction, Vol 83, pp 360-371, 2017. DOI: 10.1016/J.AUTCON.2017.06.024. Available at: www.sciencedirect.com/science/article/pii/S0926580517301139
8. B Lovelace, 'Unmanned aerial vehicle bridge inspection demonstration project', 2015. Available at: www.dot.state.mn.us/research/TS/2015/201540.pdf
9. AETOS, 'Robotic unmanned drone NDT inspections for energy'. Available at: www.aetosgroup.com/
10. N Hallermann and G Morgenthal, 'Unmanned aerial vehicles (UAV) for the assessment of existing structures', IABSE Symposium Report, Vol 101, No 14, pp 1-8, 2013. DOI: 10.2749/222137813808627172. Available at: www.ingentaconnect.com/content/iabse/report/2013/00000101/00000014/art00007
11. S K Skaga, 'Feasibility study of unmanned aerial vehicles (UAV) application for ultrasonic non-destructive testing (NDT) of wind turbine rotor blades', Master thesis, 2017. Available at: https://munin.uit.no/bitstream/handle/10037/11350/thesis.pdf?sequence=1{&}isAllowed=y
12. P B Quater, F Grimaccia, S Leva *et al*, 'Light unmanned aerial vehicles (UAVs) for cooperative inspection of PV plants', IEEE Journal of Photovoltaics, Vol 4, No 4, pp 1107-1113, 2014. DOI: 10.1109/JPHOTOV.2014.2323714
13. M Guanglei and P Haibing, 'The application of ultrasonic sensor in the obstacle avoidance of quad-rotor UAV', Proceedings of the 2016 IEEE Chinese Guidance, Navigation and Control Conference (CGNCC), Nanjing, China, pp 976-981, 12-14 August 2016. DOI: 10.1109/CGNCC.2016.7828918. Available at: http://ieeexplore.ieee.org/document/7828918/
14. J S G Guerrero, A F C González, J I H Vega *et al*, 'Instrumentation of an array of ultrasonic sensors and data processing for unmanned aerial vehicle (UAV) for teaching the application of the Kalman filter', Procedia Computer Science, Vol 75, pp 375-380, 2015. DOI: 10.1016/j.procs.2015.12.260. Available at: http://dx.doi.org/10.1016/j.procs.2015.12.260
15. Texo DSI, www.texodroneservices.co.uk
16. G Garimella and M Kobilarov, 'Towards model-predictive control for aerial pick-and-place', Proceedings of the 2015 IEEE International Conference on Robotics and Automation (ICRA), Seattle, Washington, USA, pp 4692-4697, 26-30 May 2015. DOI: 10.1109/ICRA.2015.7139850. Available at: http://ieeexplore.ieee.org/document/7139850/
17. P E Pounds, D R Bersak and A M Dollar, 'Grasping from the air: hovering capture and load stability', Proceedings of the 2011 IEEE International Conference on Robotics and Automation (ICRA), Shanghai, China, pp 2491-2498, 9-13 May 2011. DOI: 10.1109/ICRA.2011.5980314
18. C M Korpela, T W Danko and P Y Oh, 'Designing a system for mobile manipulation from an unmanned aerial vehicle', Proceedings of the 2011 IEEE Conference on Technologies for Practical Robot Applications (TePRA), Woburn, Massachusetts, USA, pp 109-114, 11-12 April 2011. DOI: 10.1109/TEPRA.2011.5753491
19. C M Korpela, T W Danko and P Y Oh, 'MMUAV: mobile manipulating unmanned aerial vehicle', Journal of Intelligent and Robotic Systems: Theory and Applications, Vol 65, No 1-4, pp 93-101, 2012. DOI: 10.1007/s10846-011-9591-3
20. F Caccavale, G Giglio, G Muscio *et al*, 'Adaptive control for UAVs equipped with a robotic arm', IFAC Proceedings Volumes, Vol 47, No 3, pp 11049-11054, 2014. DOI: 10.3182/20140824-6-ZA-1003.00790. Available at: www.sciencedirect.com/science/article/pii/S1474667016433719?via{%}3Dihub
21. A Y Mersha, S Stramigioli and R Carloni, 'Exploiting the dynamics of a robotic manipulator for control of UAVs', Proceedings of the 2014 IEEE International Conference on Robotics and Automation (ICRA), Hong Kong, China, pp 1741-1746, 31 May-7 June 2014. DOI: 10.1109/ICRA.2014.6907086. Available at: http://ieeexplore.ieee.org/document/6907086/
22. M Laiacker, F Huber and K Kondak, 'High-accuracy visual servoing for aerial manipulation using a 7 degrees of freedom industrial manipulator', Proceedings of the 2016 IEEE/RSJ International Conference on Intelligent Robots and Systems (IROS), Daejeon, South Korea, pp 1631-1636, 9-14 October 2016. DOI: 10.1109/IROS.2016.7759263. Available at: http://ieeexplore.ieee.org/document/7759263/
23. I Maza, K Kondak, M Bernard *et al*, 'Multi- UAV cooperation and control for load transportation and deployment', Journal of Intelligent and Robotic Systems, Vol 57, No 1-4, pp 417-449, 2010. DOI: 10.1007/s10846-009-9352-8. Available at: http://link.springer.com/10.1007/s10846-009-9352-8
24. J Fink, N Michael, S Kim *et al*, 'Planning and control for cooperative manipulation and transportation with aerial robots', In: Springer Tracts in Advanced Robotics (STAR), Vol 70, pp 643-659, 2011. DOI: 10.1007/978-3-642-19457-338.1003.2005
25. I Palunko, R Fierro and P Cruz, 'Trajectory generation for swing-free manoeuvres of a quadrotor with suspended payload: a dynamic programming approach', Proceedings of the 2012 IEEE International Conference on Robotics and Automation, Saint Paul, Minnesota, USA, pp 2691-2697, 14-18 May 2012. DOI: 10.1109/ICRA.2012.6225213
26. M M de Almeida and G V Raffo, 'Non-linear control of a tiltrotor UAV for load transportation', Proceedings of the 11th IFAC Symposium on Robot Control (SYROCO 2015), IFACPapersOnLine, Vol 48, No 19, pp 232-237, 2015. Available at: www.sciencedirect.com/science/article/pii/S2405896315026634
27. Z Liu, 'Modelling and control of quadrotor with tethered payload', Proceedings of the 29th Chinese Control and Decision Conference (CCDC), Chongqing, China, pp 5041-5045, 28-30 May 2017. DOI: 10.1109/CCDC.2017.7979389. Available at: http://ieeexplore.ieee.org/document/7979389/
28. M E Guerrero-Sánchez, C D García-Beltrán, D A Mercado-Ravell *et al*, 'Swing-attenuation for a quadrotor transporting a cable-suspended payload', ISA Transactions, Vol 68, pp 433-449, May 2017. DOI: 10.1016/J.ISATRA.2017.01.027. Available at: www.sciencedirect.com/science/article/pii/S0019057817301635?via{%}3Dihub
29. M Kovac, 'Learning from nature how to land aerial robots', Science, Vol 352, No 6288, pp 895-896, 2016. DOI: 10.1126/science.aaf6605. Available at: www.ncbi.nlm.nih.gov/pubmed/27199404
30. Innerspec Technologies, www.innerspec.com
31. ASTM A106/A106M – 14, 'Standard Specification for Seamless Carbon Steel Pipe for High-Temperature Service', 2014.
32. K H Brensing and B Sommer, 'Steel tube and pipe manufacturing processes', Available at: www.smrw.de/files/steel_tube_and_pipe.pdf